Journal of Power Sources 196 (2011) 2364–2372

Contents lists available at ScienceDirect

Journal of Power Sources

journal homepage: www.elsevier.com/locate/jpowsour

Synthesis and photovoltaic properties of an alternating phenylenevinylene copolymer with substituted-triphenylamine units along the backbone for bulk heterojunction and dye-sensitized solar cells

J.A. Mikroyannidis[a,*], D.V. Tsagkournos[a], P. Balraju[d], G.D. Sharma[b,c,**]

[a] Chemical Technology Laboratory, Department of Chemistry, University of Patras, GR-26500 Patras, Rion, Greece
[b] Physics Department, Molecular Electronic and Optoelectronic Device Laboratory, JNV University, Jodhpur (Raj.) 342 005, India
[c] Jaipur Engineering College, Kukas, Jaipur (Raj.), India
[d] Molecular Electronics Laboratory, JNCAR, Bangalore, India

ARTICLE INFO

Article history:
Received 17 June 2010
Received in revised form
23 September 2010
Accepted 30 September 2010
Available online 8 October 2010

Keywords:
Phenylenevinylene copolymer
Triphenylamine
Cyanoacrylic acid
Bulk heterojunction solar cells
Dye-sensitized solar cells

ABSTRACT

We have fabricated bulk heterojunction (BHJ) photovoltaic devices based on the as cast and thermally annealed **P**:[6,6]-phenyl-C-61-butyric acid methyl ester (PCBM) blends and found that these devices gave power conversion efficiency (PCE) of about 1.15 and 1.60% respectively. **P** is a novel alternating phenylenevinylene copolymer which contains 2-cyano-3-(4-(diphenylamino)phenyl)acrylic acid units along the backbone and was synthesized by Heck coupling. This copolymer was soluble in common organic solvents and showed long-wavelength absorption maximum at 390–420 nm with optical band gap of 1.94 eV. The improvement of PCE after thermal annealing of the device based on the **P**:PCBM blend was attributed to the increase in hole mobility due to the enhanced crystallinity of **P** induced by thermal treatment. In addition, we have fabricated BHJ photovoltaic devices based on the as cast and thermally annealed **PB**:**P**:PCBM ternary blend. **PB** is a low band gap alternating phenylenevinylene copolymer with BF_2–azopyrrole complex units, which has been previously synthesized in our laboratory. We found that the device based on this ternary blend exhibited higher PCE (2.56%) as compared to either **P**:PCBM (1.15%) or **PB**:PCBM (1.57%) blend. This feature was associated with the well energy level alignment of **P**, **PB** and PCBM, the higher donor–acceptor interfaces for the exciton dissociation and the improved light harvesting property of the ternary blend. The further increase in the PCE with thermally annealed ternary blend (3.48%) has been correlated with the increase in the crystallinity of both **P** and **PB**. Finally, we used copolymer **P** as sensitizer for quasi solid state dye-sensitized solar cell and we achieved PCE of approximately 3.78%.

1. Introduction

Polymer-based solar cells have emerged as a promising class of organic solar cells (OSCs) due to their low cost, light weight, mechanical flexibility, tunable electronic properties and the ease of device fabrication [1–6]. At present, power conversion efficiency (PCE) over 5% has been achieved by designing and synthesizing novel polymers as donor materials for photovoltaic (PV) applications [7–11]. Most recently, a new copolymer, PBDTTT-CF, consisting of dialkoxyl benzodithiophene and fluorine-substituted thieno[3,4-*b*]thiophene units has been synthesized and used as a donor material, and exhibits a PCE of 6.77%, when combined with [6,6]-phenyl-C71 butyric acid methyl ester (PC71BM) as acceptor [12]. Although the PCEs of polymer solar cells have improved substantially over the recent years, they remain significantly lower than those of the traditional Si-based solar cells and are still far from commercial production. One promising method for further increasing the PCE is the synthesis of low band gap donor–acceptor

Abbreviations: A, acceptor; BHJ, bulk heterojunction; CV, cyclic voltammetry; D, donor; DMF, *N*,*N*-dimethylformamide; DSSC, dye-sensitized solar cell; E_g^{opt}, optical band gap; E_{onset}^{ox}, onset oxidation; E_{onset}^{red}, onset reduction; FF, fill factor; GPC, gel permeation chromatography; HOMO, highest occupied molecular orbital; ICT, intramolecular charge transfer; IPCE, incident photon to current efficiency; ITO, indium tin oxide; *J*–*V*, current–voltage; J_{sc}, short circuit current; $\lambda_{a,max}$, long-wavelength absorption maximum; LUMO, lowest unoccupied molecular orbital; M_n, number average molecular weight; OSCs, organic solar cells; P3HT, poly(3-hexylthiophene); PC71BM, [6,6]-phenyl-C71 butyric acid methyl ester; PCBM, [6,6]-phenyl-C-61-butyric acid methyl ester; PCE, power conversion efficiency; PL, photoluminescence; PV, photovoltaic; TBP, 4-*tert*-butylpyridine; THF, tetrahydrofuran; TPA, triphenylamine; V_{oc}, open circuit voltage.

* Corresponding author. Tel.: +30 2610 997115; fax: +30 2610 997118.
** Corresponding author at: Physics Department, Molecular Electronic and Optoelectronic Device Laboratory, JNV University, Jodhpur (Raj.) 342 005, India. Tel.: +30 2610 997115; fax: +30 2610 997118.
E-mail addresses: mikroyan@chemistry.upatras.gr, mikroyan@googlemail.com (J.A. Mikroyannidis), sharmagd_in@yahoo.com (G.D. Sharma).

0378-7753/$ – see front matter © 2010 Elsevier B.V. All rights reserved.
doi:10.1016/j.jpowsour.2010.09.118

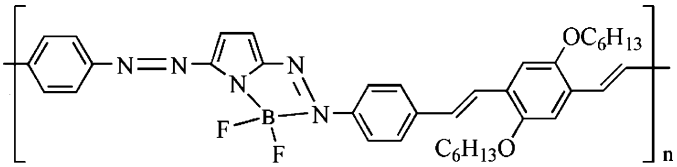

PB

Chart 1. Chemical structure of copolymer **PB**.

(D–A) polymers for use as donor materials, whose optical and electronic properties can be flexibly tuned by carefully choosing the D and A moieties [13–15,7]. When applied to OSCs, the most efficient and widely used device structure is the bulk heterojunction (BHJ), in which donor (D) and acceptor (A) components are intermixed in solution and spin-coated onto the substrate as an active layer with some degree of phase separation, providing a large D/A interface for photogenerated excitons to dissociate into free charges and an interpenetrating network for charge transport to the respective electrodes.

On the other hand, dye-sensitized solar cells (DSSCs) are currently attracting great importance because of their low cost, easy processing, and higher conversion efficiency than the conventional solid-state PV devices [16]. In these cells, dye sensitizer is one of the key components for high power conversion efficiencies. The most successful charge-transfer sensitizers employed so far in such cells are bis(tetrabutylammonium)-cis-di(thiocyanato)-*N*,*N*′-bis(4-carboxylato-4′-carboxylic acid-2,2′-bipyridine) ruthenium(II) (the N719 dye) and trithiocyanato-4,4′4″-tricaboxy-2,2′:6′,2″-terpyridine ruthenium(II) (the black dye) with an efficiency of >12% [17]. In spite of this, the main drawbacks of these sensitizers are the lack of absorption in the red region of the visible spectrum as well as rarity of the metal in the earth crust. As Ru dyes are exclusive, metal-free organic molecules, tetrapyrrolic compounds such as porphyrins and phthalocyanines are potential alternative sensitizers for DSSC applications based on their thermal as well as electronic properties [18].

Triphenylamine (TPA) is a unique molecule possessing 3D propeller-like geometry, glass-forming property, and relatively high oxidation potential as well as excellent hole-transporting property. A literature survey revealed that various TPA-based materials have been used for BHJ solar cells very recently [19–26]. Moreover, theoretical and experimental studies have demonstrated that the TPA unit, which suppresses the dye aggregation for its nonplanar structure, can be used as the sensitizer of DSSCs [27]. Very recently, a few groups [28–33] have reported that DSSCs with various triphenylamine-based dyes have shown PCEs up to ~7% under AM 1.5 irradiation, indicating the importance of their further investigation in this topic.

The present investigation describes the synthesis and characterization of a novel alternating phenylenevinylene copolymer **P** which contains substituted TPA units along the backbone and solubilizing hexyloxy side chains. The TPA is connected to the cyanoacrylic acid through a methine bridge. The copolymer **P** was successfully synthesized by Heck coupling. This copolymer was used as donor for BHJ solar cells with [6,6]-phenyl-C-61-butyric acid methyl ester (PCBM) as acceptor. The PCE for the BHJ device based on the as cast and thermally annealed **P**:PCBM blend is about 1.15% and 1.60%, respectively. The increase in the PCE for the thermally annealed blend was attributed to the raise in hole mobility due the enhanced crystallinity of **P** in the blend. In addition, the ternary blend **P**:**PB**:PCBM (as cast and annealed) was used for BHJ solar cells. **PB** is a low band gap alternating phenylenevinylene copolymer with BF_2–azopyrrole complex units (Chart 1). Copolymer **PB** has been previously synthesized in our laboratory and used for BHJ solar cells. In particular, the **PB**:PCBM BHJ devices have given PCE 1.57% and 3.25% for the as cast and thermally annealed film respectively [34]. Certain photophysical characteristics of **PB** are listed in Table 1. The BHJ device based on the **PB**:**P**:PCBM ternary blend exhibited improved PCE (2.56 and 3.48% for the as cast and thermally annealed blend) as compared to the devices based on either **P**:PCBM or **PB**:PCBM blends. This effect has been interpreted in terms of improved light harvesting property of ternary blend, increased D/A interfaces for the exciton dissociation and proper energy level alignment of **P**, **PB** and PCBM. The increase in the PCE for the device based on the thermally annealed ternary blend has been attributed to the improved crystallinity of both **P** and **PB**, which leads to an increase in the hole mobility and better balance charge transport. Besides, since copolymer **P** contains cyanoacrylic acid anchoring groups, we used it as photosensitizer for quasi solid state DSSCs cells and we achieved PCE of ~3.78%.

Table 1
Photophysical and electrochemical properties of copolymers **P** and **PB**.

Copolymer	**P**	**PB**
$\lambda_{a,max}$[a] in solution (nm)	390	434
$\lambda_{a,max}$[a] in thin film (nm)	420 (435)[d]	511
Thin film absorption onset (nm)	640	763
E_g^{opt} (eV)[b]	1.94	1.63
E_{onset}^{ox} (V)	0.75	0.40
E_{onset}^{red} (V)	−1.25	−1.25
HOMO (eV)	−5.45	−5.10
LUMO (eV)	−3.45	−3.45
E_g^{el} (eV)[c]	2.00	1.65

[a] $\lambda_{a,max}$: the long-wavelength absorption maxima from the UV–vis spectra in THF solution or in thin film.
[b] : optical band gap determined from the absorption onset in thin film.
[c] : electrochemical band gap determined from cyclic voltammetry.
[d] The long-wavelength absorption maximum of thin film after thermal annealing at 120 °C for 2 min.

2. Experimental

2.1. Reagents and solvents

1,4-Divinyl-2,5-bis(hexyloxy)-benzene was prepared by Stille coupling reaction [35] of 1,4-dibromo-2,5-bis(hexyloxy)-benzene with tributylvinyltin [36]. Triethylamine was purified by distillation over KOH. *N*,*N*-Dimethylformamide (DMF) and tetrahydrofuran (THF) was dried by distillation over CaH_2. All other reagents and solvents were commercially purchased and were used as supplied.

2.2. Synthesis of compounds and copolymer

2.2.1. 4-(Diphenylamino)benzaldehyde (*1*)

This compound was synthesized by formylation of TPA using DMF and $POCl_3$ according to the reported method [37].

2.2.2. 4-(Bis(4-bromophenyl)amino)benzaldehyde (*2*)

This compound was synthesized by bromination of **1** in dichloromethane according to the reported method [37].

2.2.3. (E)-3-(4-(Bis(4-bromophenyl)amino)phenyl)-2-cyanoacrylic acid (*3*)

A flask was charged with a mixture of **2** (0.3470 g, 0.805 mmol), cyanoacetic acid (0.0850 g, 0.966 mmol), glacial acetic acid (7 mL) and a catalytic amount of ammonium acetate. The mixture was stirred and refluxed under nitrogen for 24 h. The reaction solution became red during the heating. Then it was concentrated under reduced pressure and water was added to the concentrate. The yellow-brown solid thus obtained was filtered, pulverized, washed

thoroughly with water and dried to afford **3**. It was purified by recrystallization from ethanol (0.36 g, 90%).

FT-IR (KBr, cm^{-1}): 3340–3200 (O–H stretching of carboxyl); 2216 (cyano); 1700 (C=O stretching of carboxyl); 1314 (C–N stretching of TPA); 3031, 1576, 1506 (aromatic).

^{1}H NMR (DMSO-d_6) ppm: 12.00 (br, 1H, carboxyl); 8.00 (s, 1H, cyanovinylene); 7.88 (m, 2H, TPA ortho to cyanoacrylic acid); 7.42 (m, 4H, TPA ortho to bromine); 7.23 (m, 6H, TPA ortho to nitrogen).

Anal. Calcd. for $C_{22}H_{14}Br_2N_2O_2$: C, 53.04; H, 2.83; N, 5.62. Found: C, 52.86; H, 2.67; N, 5.43.

2.2.4. Copolymer P

A flask was charged with a mixture of **3** (0.1367 g, 0.274 mmol), 1,4-divinyl-2,5-bis(hexyloxy)-benzene (0.0907 g, 0.274 mmol), $Pd(OAc)_2$ (0.0026 g, 0.012 mmol), P(*o*-tolyl)$_3$ (0.0192 g, 0.063 mmol), DMF (8 mL) and triethylamine (3 mL). The flask was degassed and purged with N_2. The mixture was heated at 90 °C for 24 h under N_2. Then, it was filtered and the filtrate was poured into methanol. The precipitate was filtered and washed with methanol. The crude product was purified by dissolving in THF and precipitating into methanol (0.14 g, yield 76%).

FT-IR (KBr, cm^{-1}): 3340–3200 (O–H stretching of carboxyl); 2952, 2926 (C–H stretching of hexyloxy); 2212 (cyano); 1697 (C=O stretching of carboxyl); 1284, 1070, 1008 (ether bond); 1314 (C–N stretching of TPA); 3030, 1592, 1506 (aromatic); 966 (trans vinylene bond).

^{1}H NMR ($CDCl_3$) ppm: 12.00 (br, 1H, carboxyl); 8.05 (s, 1H, cyanovinylene); 7.90 (m, 2H, TPA ortho to cyanoacrylic acid); 7.43 (m, 4H, TPA ortho to vinylene); 7.25–7.12 (m, 6H, TPA ortho to nitrogen, and 4H vinylene); 6.82 (s, 2H, phenylene ortho to oxygen); 3.95 (m, 4H, $OCH_2(CH_2)_4CH_3$); 1.82 (m, 4H, $OCH_2CH_2(CH_2)_3CH_3$); 1.36 (m, 12H, $O(CH_2)_2(CH_2)_3CH_3$); 0.92 (t, J = 5.4 Hz, 6H, $O(CH_2)_5CH_3$).

Anal. Calcd. for $(C_{44}H_{46}N_2O_4)_n$: C, 79.25; H, 6.95; N, 4.20. Found: C, 78.92; H, 6.87; N, 4.13.

2.3. Characterization methods

IR spectra were recorded on a Perkin-Elmer 16PC FT-IR spectrometer with KBr pellets. ^{1}H NMR (400 MHz) spectra were obtained using a Brucker spectrometer. Chemical shifts (δ values) are given in parts per million with tetramethylsilane as an internal standard. UV–vis spectra were recorded on a Beckman DU-640 spectrometer with spectrograde THF. Elemental analyses were carried out with a Carlo Erba model EA1108 analyzer. Gel permeation chromatography (GPC) analysis was conducted with a Waters Breeze 1515 apparatus equipped with a 2410 differential refractometer as a detector (Waters Associate) and Styragel HR columns with polystyrene as a standard and tetrahydrofuran (THF) as an eluent.

2.4. Device fabrication and characterization

First copolymer **P** was well dissolved in THF solution with a concentration of 10 mg mL^{-1} and then it was mixed with the PCBM solution in THF (10 mg mL^{-1}). The resulting mixture was used to prepare the **P**:PCBM blend film. The weight ratio of **P** and PCBM in the blend is 1:1. For the ternary blend, the above mixture was mixed with the **PB** solution in THF (10 mg mL^{-1}) and the resulting mixture was used to prepare the **P**:**PB**:PCBM (1:1:1 by weight) ternary blend thin film. The polymer PV devices were prepared in a glove box, on indium tin oxide (ITO) coated glass substrates. The substrates were cleaned in an ultrasonic bath with water and acetone. After cleaning the substrate, the PEDOT:PSS layer was spin coated with a thickness of about 80 nm and baked at 80 °C for 30 min in an oven. The 80–90 nm thick photoactive layer (**P**:PCBM or **P**:**PB**:PCBM) was spin coated from the above prepared blend solutions on the top of the PEDOT:PSS layer for 1 min. The thickness of the active layer was adjusted by tuning the spin coating rate. Finally, an Al electrode was deposited by the vacuum thermal evaporation method on top of the photoactive layer to form the ITO/PEDOT:PSS/**P**:PCBM or **P**:**PB**:PCBM/Al structure. The active area of the device is 5 mm^2. For thermal annealing, the photoactive layer was thermally annealed at temperature of 120 °C for 2 min, before the deposition of the Al electrode.

The current–voltage (J–V) characteristics of the devices in dark and under illumination were measured by a semiconductor parameter analyzer (Keithley 4200-SCS). A xenon lamp source (Oriel USA) was used to give the simulated irradiance of 100 mW cm^{-2} (equivalent to AM 1.5 irradiation) at the surface of the device. The photoaction spectra of the devices were measured using a monochromator (Spex 500 M, USA) and the resulting photocurrent was measured with a Keithley electrometer (model 6514), which is interfaced to the computer by LABVIEW software.

2.5. Fabrication of polymer sensitized solar cells

TiO_2 paste was prepared by slowly adding 1 g of TiO_2 powder (P25 Degussa) to a mixture of 0.2 mL acetic acid, 1 mL of water, and 60 mL of ethanol. Then this mixture was sonicated for 3 h. Finally Triton X-100 was added and the well dispersed colloidal paste was coated over the FTO glass by the doctor blade technique. The TiO_2 coated FTO electrode was sintered at 450 °C for 30 min. Copolymer **P** was dissolved in THF solution and the TiO_2 electrode was immersed into this solution for 12 h and after the sensitization, the electrode was washed. The thickness of the copolymer sensitized TiO_2 layer is about 20 μm. Quasi solid state polymer electrolyte was prepared by adding 0.083 g of P25 TiO_2 powder, 0.1 g of LiI, 0.019 g of I_2, 0.264 g of PEO, and 44 μL of 4-*tert*-butylpyridine (TBP) to a (1:1) acetone/propylene carbonate solution. Finally, the electrolyte was spin coated over the polymer sensitized TiO_2 electrode.

To prepare the platinum counter electrode, H_2PtCl_4 solution in iso-propanol (2 mg mL^{-1}) was deposited onto the FTO glass substrates and sintered at 400 °C for 30 min. The polymer sensitized quasi solid state solar cell was fabricated by sandwiching the electrolyte between the polymer sensitized TiO_2 photoanode and the counter electrode. The effective area of the DSSC is 0.25 cm^2. The J–V characteristics of the device were measured by the same method as described for BHJ solar cells.

3. Results and discussion

3.1. Synthesis and characterization

Copolymer **P** was synthesized by a four-step reaction sequence which is outlined in Scheme 1. In particular, compounds **1** [37] and **2** [37] were synthesized following the reported procedures. The condensation of **2** with cyanoacetic acid in glacial acetic acid in the presence of a catalytic amount of ammonium acetate afforded compound **3**. Finally, the Heck coupling of **3** with 1,4-divinyl-2,5-bis(hexyloxy)-benzene in DMF utilizing Et_3N as acid scavenger and $Pd(OAc)_2$ as catalyst gave copolymer **P**. The crude product was purified by dissolution in THF and precipitation into methanol. This copolymer displayed enhanced solubility in common organic solvents like THF, dichloromethane and chloroform due to the hexyloxy side chains and the nonplanar configuration of the TPA segment. Copolymer **P** had number average molecular weight (M_n) of 8600, by GPC, with a polydispersity of 2.3.

The FT-IR spectrum of **P** showed characteristic absorption bands at 3340–3200 (O–H stretching of carboxyl); 2952, 2926 (C–H stretching of hexyloxy); 2212 (cyano); 1697 (C=O stretching of

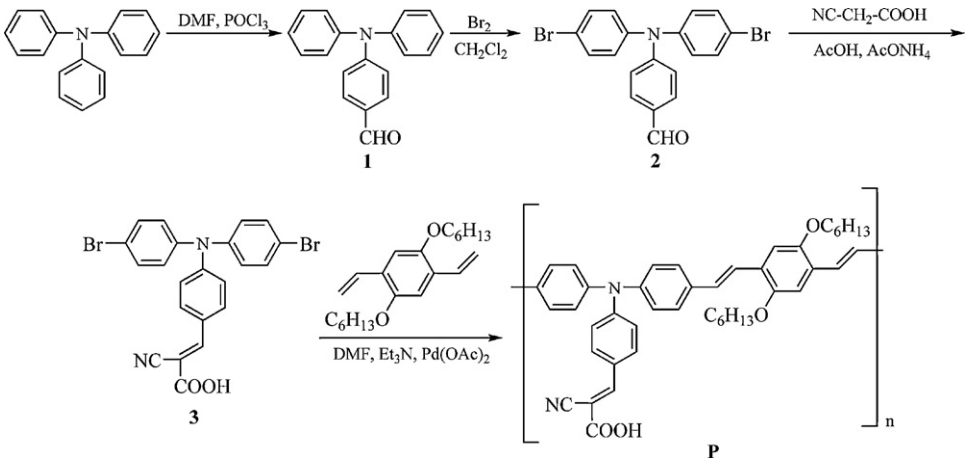

Scheme 1. Synthesis of copolymer **P**.

carboxyl); 1284, 1070, 1008 (ether bond); 1314 (C–N stretching of TPA); 3030, 1592, 1506 (aromatic) and 966 cm^{-1} (trans vinylene bond). The ^1H NMR spectrum of **P** displayed upfield signals at 12.00 (carboxyl) and 8.05 ppm (cyanovinylene). The signals at 7.90 and 7.43 ppm were assigned to the TPA protons ortho to cyanoacrylic acid and ortho to vinylene respectively. The TPA protons ortho to nitrogen were overlapped with the vinylene protons at 7.25–7.12 ppm, while the phenylene protons ortho to oxygen gave peaks at 6.82 ppm. Finally, the aliphatic protons of the hexyloxy chains resonated at the range of 3.95–0.92 ppm.

3.2. Photophysical properties

Fig. 1 depicts the UV–vis absorption spectra of copolymer **P** in both dilute (10^{-5} M) THF solution and thin film, while Table 1 summarizes all photophysical characteristics of copolymers **P** and **PB**. The absorption spectra of **P** were broad and extended from 300 up to ~650 nm. They displayed long-wavelength absorption maximum ($\lambda_{a,max}$) at 390 nm in solution and 420 nm in thin film. Moreover, both absorption spectra showed a shoulder approximately at 476 nm. The $\lambda_{a,max}$ at 390 and 420 nm was assigned to an intramolecular charge transfer (ICT) between the TPA/dialkoxyphenylene donor and the cyanoacrylic acid acceptor [38]. Similar absorptions have been observed in other TPA-containing dyes which have been used for DSSCs [39]. After thermal annealing of the thin film at 120 °C for 2 min, the $\lambda_{a,max}$ was red-shifted by 15 nm and appeared at 435 nm, while the shoulder at 476 nm became more distinct (Fig. 1). The red shift of the main absorption peak and the distinct vibronic shoulder of annealed film, compared to as cast film, was attributed to a higher degree of crystallinity induced by thermal annealing. Interestingly, the solution absorption onset was almost the same with that in thin film which indicates that there is not any stacked aggregation in solid state due to the non-planar structure of the TPA unit. The thin film absorption onset was located at 640 nm corresponding to an optical band gap (E_g^{opt}) of 1.94 eV. The optical bang gap of **P** (1.94 eV) is almost the same with that of poly(3-hexylthiophene) (P3HT). This suggests that copolymer **P** can be used as electron donor for BHJ PV devices with PCBM as electron acceptor.

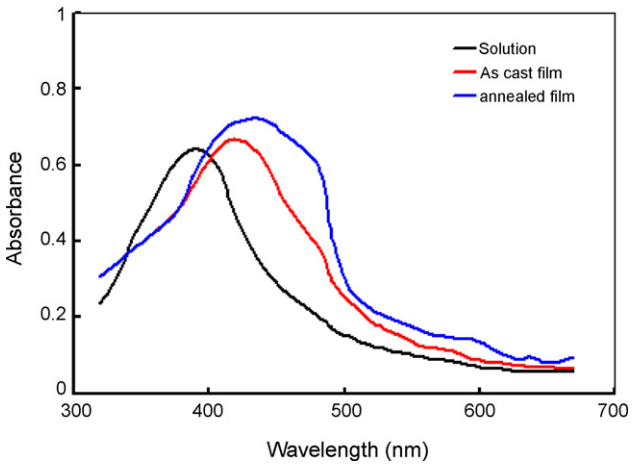

Fig. 1. UV–vis spectra of copolymer **P** in THF solution and thin film as cast and after thermal annealing at 120 °C for 2 min.

Cyclic voltammetry (CV) is employed to calculate the oxidation and reduction potentials, the highest occupied molecular orbital (HOMO) and the lowest unoccupied molecular orbital (LUMO) energy levels of **P**. The potentials have been measured with respect to the Ag/Ag^+ electrode. HOMO and LUMO levels were calculated from the following equations:

$$E_{HOMO}(eV) = -e[E_{onset}^{ox}(V) + 4.7] \quad \text{and}$$

$$E_{LUMO}(eV) = -e[E_{onset}^{red}(V) + 4.7]$$

where E_{onset}^{ox} and E_{onset}^{red} are the onset oxidation and reduction potentials observed in the cyclic voltammogram. The electrochemical values are compiled in Table 1. The HOMO and LUMO levels of **P** are −5.45 eV and −3.45 eV, respectively. The electrochemical band gap (2.00 eV) is larger than the optical band gap (1.94 eV), as usually observed in other conjugated polymers. The difference between the LUMO levels of **P** and PCBM (−4.0 eV) is approximately 0.55 eV, which indicates that the combination of **P** as a donor with PCBM as an acceptor can be used for BHJ polymer solar cells.

3.3. Charge carrier mobility of copolymer P

We have measured the *J–V* characteristics of the ITO/PEDOT:PSS/**P**/Au device in dark to estimate the hole mobility of copolymer **P**. Since the HOMO level of **P** is close to both HOMO level of PEDOT:PSS and work function of Au, we assume that under forward bias (PEDOT:PSS/ITO electrode is positive with respect to Au electrode), both interfaces (Au/P and ITO/PEDOT:PSS/P) form the nearly Ohmic contact in the device. The device acts as hole only device. The *J–V* data were analyzed using nonlinear square fitting

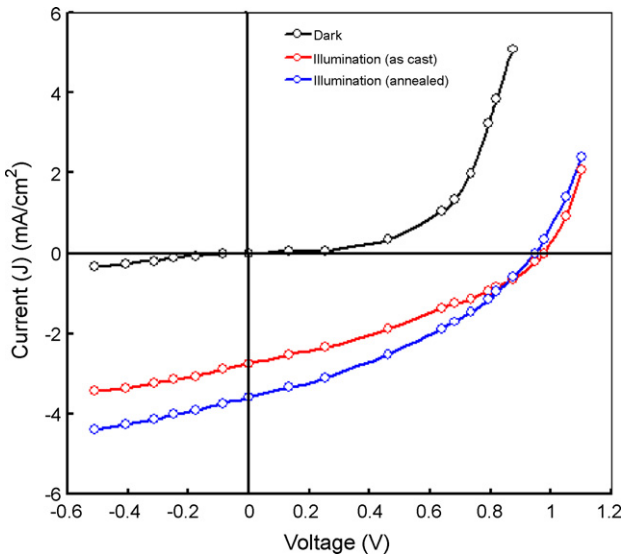

Fig. 2. Current–voltage characteristics of ITO/PEDOT:PSS/**P**:PCBM/Al devices in dark and under illumination intensity of 100 mW cm^{-2}.

to the modified Mott–Gurnay equation, described as:

$$J = \frac{9}{8}\varepsilon\varepsilon_0\mu\frac{V^2}{L^3}\exp\left(0.89\beta\sqrt{\frac{V}{L}}\right)$$

where J is the current density, V is the applied voltage, L is the thickness of the active layer, μ is the zero field mobility, ε is the dielectric constant, ε_0 is the permittivity of free space (8.85×10^{-12} F m^{-1}) and β is the field activation factor. From the analysis of the J–V curve in dark and using the above equation, the zero field mobility of the as cast and thermally annealed **P** were determined to be 1.2×10^{-5} and 3.3×10^{-5} cm^2 V^{-1} s^{-1}, respectively. The increase in the hole mobility for the thermally annealed **P**, was attributed to the enhanced crystallinity of **P** as it has been shown in the absorption spectra of this copolymer.

3.4. Photovoltaic properties of *P*:PCBM blend device

We have used copolymer **P** as electron donor with PCBM as electron acceptor for BHJ PV devices. The J–V characteristics of the device in dark and AM 1.5 irradiation (100 mW cm^{-2}) are shown in Fig. 2. The device ITO/PEDOT:PSS/**P**:PCBM/Al shows a rectification effect in dark. The optimized PV parameters are listed in Table 2. We have observed quite high open circuit voltage (V_{oc}) for this device, which is attributed to the large difference between the LUMO of PCBM and HOMO of **P**. In a BHJ device, if both electrodes form the Ohmic contact with the photoactive layer, the open circuit is mainly governed by the difference between the LUMO level of acceptor and the HOMO level of donor used in the device [40]. The HOMO level of PEDOT:PSS (−5.1 eV) almost matches with the HOMO level of **P** (−5.45 eV), resulting in nearly Ohmic contact for holes in the device, under forward bias conditions. On the other hand, the Al makes nearly Ohmic contact for electron injection from Al into the LUMO of PCBM. For this case the V_{oc} is given by [40]

$$q(V_{oc} - \Delta V_b) = (\text{HOMO})_{\text{donor}} - (\text{LUMO})_{\text{acceptor}}$$

where ΔV_b is the sum of the voltage losses at each contact due to the band bending. For the ideal case, the theoretical value of V_{oc} of the device using **P**:PCBM blend should be 1.45 V. But the experimental value of V_{oc} is about 0.98 V, which is lower by 0.47 V than the theoretical value. This may be attributed to the voltage losses at the interfaces, due the mismatching of the HOMO of **P** and the LUMO of PCBM with the energy levels of PEDOT:PSS and Al electrodes, respectively.

The values of short circuit current (J_{sc}) and fill factor (FF) are 2.73 mA cm^{-2} and 0.43, respectively resulting PCE of ~1.15% which is lower than that for other conjugated polymers having a similar band gap. We assume that this lower PCE may be a result of the low hole mobility of **P** and charge carrier losses at the interfaces, due to the unbalanced charge transport, which leads to the formation of space charge at the interface. As it can be seen from Table 2, the PCE of the device based on the thermally annealed **P**:PCBM blend has been increased up to 1.54%. The increase in the PCE may be attributed to the raise in hole mobility and enhanced crystallinity of the **P** in **P**:PCBM blend.

3.5. Photovoltaic properties of the *P*:*PB*:PCBM ternary blend

Recently, the energy harvesting capabilities of OSCs have been improved through the use of low band gap conjugated polymers [41]. Although the absorption spectra of these polymers are extended into the long-wavelength region (e.g., near infrared), they still sacrifice some absorption in the visible region. Moreover, the offsets of the HOMO levels of the donors and acceptors lead to significant losses upon exciton dissociation. Therefore, to enhance photocurrent generation, great interest remains in combining organic semiconductors that exhibit complementary spectra.

We have investigated an approach to enhance the spectroscopic response of **P**:PCBM by blending this with a low band gap conjugated copolymer **PB**. We found that the low band gap copolymer **PB**, whose electronic levels are well aligned with the electrochemically determined potentials of **P** and PCBM, whose potential for application in organic PVs has been investigated earlier [34], efficiently contributes to photocurrent generation in longer wavelength region of the spectrum. The charge transport mechanism and sensitization effect of **PB** with **P**:PCBM blend on PV response are investigated by both J–V characteristics in dark and under illumination and IPCE spectra of the device. The transfer of positive charge from both **PB** to **P** and **P** to **PB** is found to be the dominant process which leads to a design rule for the ternary systems, where copolymers **PB** and **P** act as light absorber and charge transporter, respectively.

Copolymer **PB** with smaller band gap (E_g = 1.65 eV) has broader absorption feature in comparison to copolymer **P** (E_g = 1.94 eV). Besides the absorption peak at 525 nm, **PB** exhibits vibronic features at longer wavelength around 630–640 nm. These features, which are originally absent in the absorption profile of **PB** in solution, indicate the presence of strong interchain π–π interactions due to the high degree of crystallinity in the blend, as it has been also reported for P3HT [42].

Table 2
Photovoltaic parameters of BHJ devices based on binary and ternary blended films.

Blends	Short circuit current (J_{sc}) (mA cm^{-2})	Open circuit voltage (V_{oc}) (V)	Fill factor (FF)	Power conversion efficiency (η) (%)
P:PCBM (as cast)	2.73	0.98	0.43	1.15
P:PCBM (annealed)	3.60	0.95	0.47	1.60
PB:PCBM (as cast) [34]	3.80	0.86	0.48	1.57
PB:**P**:PCBM (as cast)	5.60	0.88	0.52	2.56
PB:**P**:PCBM (annealed)	7.50	0.86	0.54	3.48

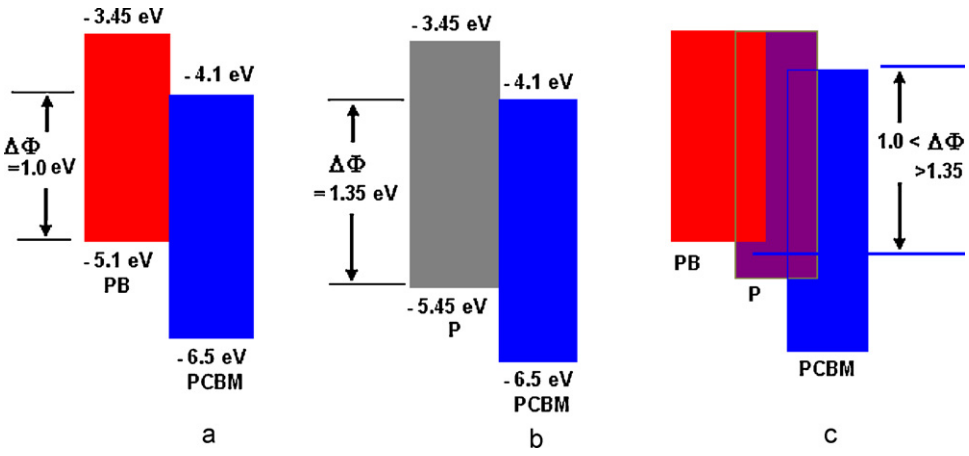

Fig. 3. Flat energy band diagrams for binary BHJ (a) **PB**:PCBM, (b) **P**:PCBM and (c) **PB**:**P**:PCBM ternary BHJ. $\Delta\Phi$ denotes the offset energy between the HOMO of electron donor (**PB** or **P**) and the LUMO of the electron acceptor (PCBM).

PB has been used as a donor copolymer in conjugation with the **P**:PCBM blend for two reasons. Its absorption spectrum extends into longer wavelength region. It is thus complementary to copolymer **P**, which has absorption maximum around 420 nm, where **PB** has an absorption minimum. The criteria for the selection of **P**:PB:PCBM are the positions of the electronic energy levels of **P**, **PB** and PCBM. Table 1 displays the HOMO and LUMO levels of **P**, **PB** as determined by CV. The HOMO level of **P** is located between the HOMOs of **PB** and PCBM (as shown in Fig. 3). The LUMO levels for **P** and **PB** are almost the same. As a consequence, photoinduced charge transfer is energetically allowed between **P** and PCBM, between **PB** and PCBM, as well as between **P** and **PB**. The key parameters, to improve the PCE of polymer solar cells are the control of nanoscale morphology and light harvesting property of the photoactive blend layer [43]. The competing processes which are strongly reliant on blend morphology are exciton dissociation and charge transport. To maximize the dissociation of photogenerated excitons, a larger D/A interfacial area should be achieved.

From the electronic point of view, one important effect is that the band gap of **PB** is about 0.30 eV smaller than that for **P**. This implies that the **PB** will be more appropriate for harvesting light in the red and infrared parts of the sun's spectrum. Charge mobility will also depend on the interaction between neighboring chains [44] and in fact, hole mobility of **P** (1.2×10^{-5} cm^2 V^{-1} s^{-1}) is lower than that of **PB** (4.6×10^{-5} cm^2 V^{-1} s^{-1}) [34]. Consequently, in order to ensure good charge generation (and J_{sc}) in OPVs based on ternary systems, the amount of **P** should, theoretically, be smaller compared to **PB**.

The flat energy band diagram of the ternary system is shown in Fig. 3. Considering the energy band diagram, the V_{oc} in the present ternary blend (**PB**:**P**:PCBM) device configuration is expected to be improved when the **P** component directly contacts the PEDOT:PSS. This assumption is based on the report that the trend of V_{oc} in organic solar cells is ideally determined by the offset energy between the HOMO of the electron donating component (here **P** or **PB**) and the LUMO of the electron-accepting component (here PCBM).

Fig. 4 displays the *J*–*V* characteristics of the devices based on the as cast and thermally annealed **PB**:**P**:PCBM ternary blends, in dark and under illumination intensity of 100 mW cm^{-2}. The device shows good rectification effect indicating the formation of a BHJ device. The PV parameters are summarized in Table 2. The device based on **PB**:**P**:PCBM ternary blend exhibits V_{oc} value about 0.88 V, which is the intermediate value of two binary blend devices that is slightly close to the **PB**:PCBM device. This implies that the **PB** component in the ternary blend device became relatively richer in the direction of PEDOT:PSS. The J_{sc} in the device based on ternary blend is higher than that for both devices based on either **P**:PCBM or **PB**:PCBM binary blend. The photocurrent in the device based on **P**:**PB**:PCBM blend is induced by the light absorption of both **P** and **PB** and followed by the excitons creation. These excitons diffuse to the D/A interfaces, where they can dissociate into free carriers depending upon the strength of the local electric field that results from the difference between the LUMO levels of **P** or **PB** and PCBM. Therefore, the interfacial electric field drives the charge separation effectively and generated electrons are transported through PCBM towards Al electrode, while the holes are transported through both **P** and **PB** towards PEDOT:PSS electrode. The steepest slope of the *J*–*V* curves at the forward voltage above the V_{oc} observed for the device based on ternary blend indicates the lowest charge blocking resistance for this device [45].

The charge carrier mobility study of the devices with ternary blend (as cast and thermally annealed) was conducted with hole and electron only devices using the space charge limited current methods [46]. The hole mobility for the as cast **P**:PCBM and **PB**:**P**:PCBM blends is about 0.98×10^{-6} cm^2 V^{-1} s^{-1} and 4.6×10^{-5} cm^2 V^{-1} s^{-1}, respectively. Hence, the increase in the hole mobility also contributes to the enhancement in the J_{sc} for ternary blend device as compared to binary blend device. Thermal annealing fur-

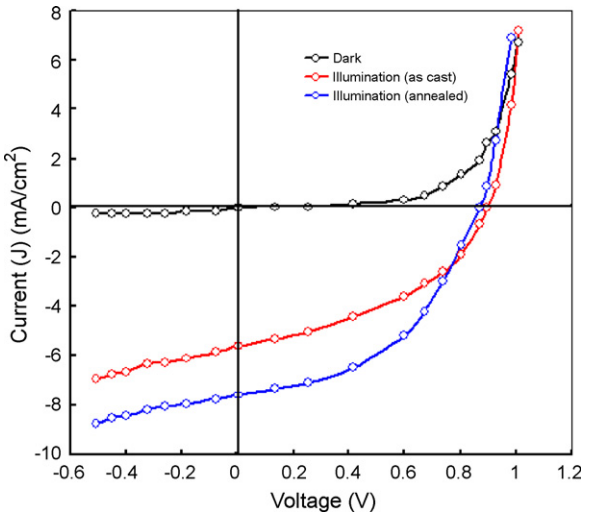

Fig. 4. Current–voltage characteristics of ITO/PEDOT:PSS/**PB**:**P**:PCBM/Al devices in dark and under illumination intensity of 100 mW cm^{-2}.

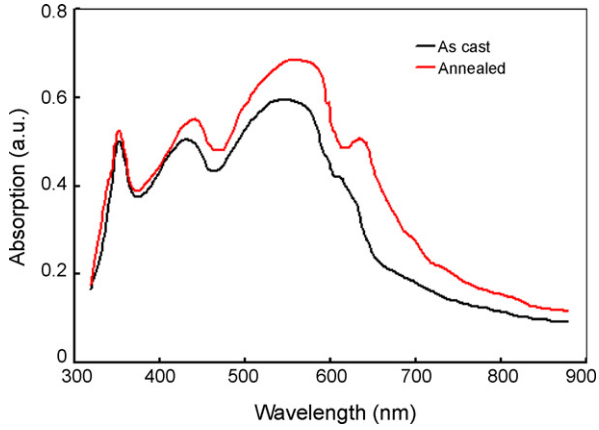

Fig. 5. . UV–vis spectra of the as cast and thermally annealed at 120 °C for 2 min **PB**:**P**:PCBM blend.

ther increases the hole mobility up to 6.1×10^{-5} cm^2 V^{-1} s^{-1}, which also enhances the PCE of the device up to 3.48% due to the increased crystallinity of both copolymer **P** and **PB**. Thus, more balanced hole/electron mobility and lower internal resistance as a result of ternary blend, are likely expected to contribute to the increase in FF and hence the PV performance of the device.

Thermal annealing is employed to trigger reorganization of the **P** and **PB** in the blend to a more crystalline structure. The optical absorption spectra of ternary blend film before and after thermal annealing are shown in Fig. 5. The major effect of thermal annealing on the blend film is the shifting of the absorption peaks towards the longer wavelengths. The absorption peaks around 440 nm and 510 nm observed in the blend before thermal annealing correspond to **P** and **PB**, respectively. These peaks are red shifted upon thermal annealing. Consequently, the large red shift of P, in contrast to the small red shift of **PB** peak, resulted in a broadening of the absorption wavelength range of the **P**:**PB**:PCBM blend film. Therefore, the ternary blend annealed at 120 °C, increases the absorbed photons through the broadening of the absorption wavelength range occurring by thermal annealing. The effect of thermal annealing on the blend film, which appears as a red shift of the absorption peaks of both **P** and **PB**, can be explained by the basis of the structure organization of both **P** and **PB** chains, which are well known to crystallize upon thermal annealing, as has been reported for other conjugated polymers [47]. After thermal annealing, the part of absorption spectra originating from the ordered phase is red shifted. This is in agreement with the crystal growth theory of polymers, which states that with the increase of temperature, the size of crystallites increases. As the polymer chains are extended through the crystallites, the thicker crystallites would give a longer conjugation length [48]. The overall red shift in the absorption of blend film by thermal annealing is an indication of increasing conjugation length in the blend. This means that the alternation of single–double bonds between the carbon atoms increases, and therefore, the π–π^* transition shifts to lower energy. This tends to result in a decrease in the energy band gap of the blend by thermal annealing. Therefore, by thermal annealing, the blend absorbs a large amount of photons, which have lower energy, and consequently the generation of charge carriers, may be increased in the solar cell. The improvement in the ternary blend with thermal annealing may result in a positive impact on the J_{sc}. The heat treatment facilitates the reorganization of the copolymers to a more thermodynamically stable state. The absorption profile of the heat treated blend exhibits a distinct shoulder peak around 610–615 nm, while an increase in the intensity is observed at absorption near 510 nm peak. Since, both PCBM and P have no significant absorption above 450 nm, this shoulder peak is attributed to reorganization of PB chains into crystallites.

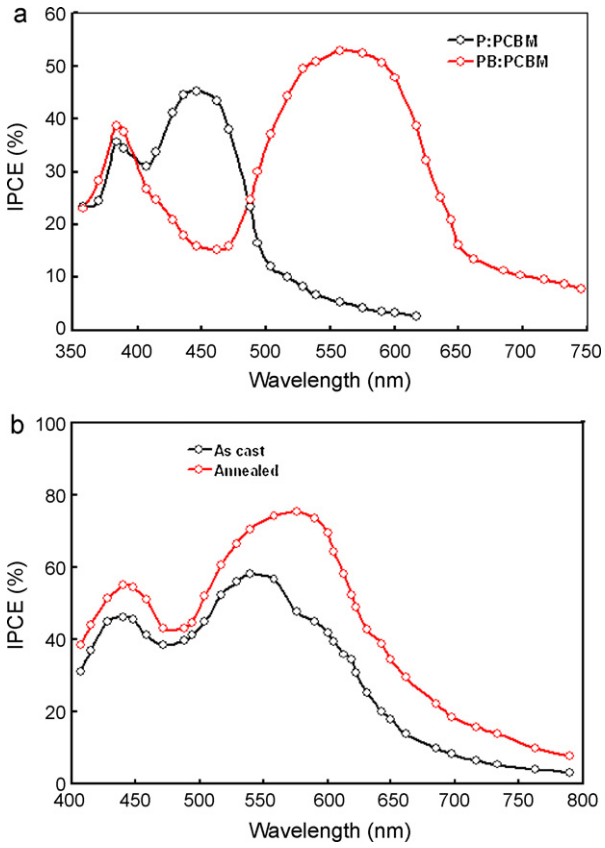

Fig. 6. IPCE spectra of BHJ photovoltaic devices based on (a) **P**:PCBM and **PB**:PCBM, (b) as cast and thermally annealed ternary **PB**:**P**:PCBM blend.

Thermal annealing facilitates the diffusion of copolymers and their phase separation, enhancing the interchain π–π interaction of PB chains, and eventually improving the absorption of blend around 480–650 nm, as has been reported for other conjugated polymer blend with PCBM [49].

The thermal treatment is found to affect the J_{sc} significantly, which depends strongly on various factors, such as the amount of photons absorbed, efficiency of exciton dissociation and effectiveness of free charge carrier transport. The increase in J_{sc} can be attributed to the improved degree of crystallinity that results in enhanced absorption and charge transport. As shown in the photoluminescence (PL) study, the improved charge transport is one of the contributing factors to the PL quenching in the blend films. The reduction in the V_{oc} is attributed to the decrease in the HOMO level of the donor due to the increase in crystallinity [50]. The low value of FF in OSC may indicate an imbalance between hole and electron transport and poor morphology. The difference in the charge mobility induces build up of the space charge region, which can impede charge extraction by the electrodes, increasing the internal resistance in the blend [51]. The improvement in hole mobility induced by the thermal annealing reduces the imbalance in the charge transport, leading to in enhancement in the FF.

The IPCE spectra of the devices based on the as cast and thermally annealed **P**:**PB**:PCBM blends are shown in Fig. 6(b). The IPCE spectra of the **P**:PCBM and **PB**:PCBM are also shown in Fig. 6(a). It can be seen from these figure that the IPCE spectra of the **P**:**PB**:PCBM blend is the sum of the **P**:PCBM and **PB**:PCBM blends. The IPCE profile is similar to the absorption spectra of the ternary blend, indicating that the overall photocurrent is stemmed from the absorption of both **PB** and **P** copolymers. The increase in IPCE for the device based on the thermally annealed ternary blend as compared to the as cast based device has been attributed to the

improved light harvesting property of the annealed blend and better charge transport in the device. This observation is in consistence with the value observed for J_{sc}.

The improvement in the PV performance is consistent with the thermally activated molecular organization observed in the optical absorption spectrum of the annealed ternary blend thin film. The IPCE increases significantly after the thermal annealing. In particular, a considerable amount of current is produced in the absorption region of **P**:**PB** blend. This enhancement in photocurrent and IPCE can also be explained by an increase in hole mobility in the annealed active blend layer. We believe that in the BHJ device based on the annealed blend, the improvement of the PV performance is due to the better copolymer chain ordering within thin film, allowing charge transport. The high PCE could be attributed to the thermally induced modification of morphology, i.e. thermally induced crystallization and improved charge transport across the interface between BHJ materials and PEDOT:PSS/ITO electrode.

3.6. Quasi solid state DSSCs based on copolymer P

The widely used dyes are Ru complexes, which involve a rare metal with low yield. Great efforts have been devoted to replacing Ru complex dyes with metal free organic dyes [52]. The advantages of sufficiently large absorption coefficient, tunable energy levels and easy deposition at various substrates make conjugated polymers promising candidates as organic sensitizers in DSSCs. The application of conjugated polymers as sensitizers in DSSCs have been reported recently [53]. Although the DSSCs based on liquid electrolyte have already afforded a PCE of 10.6%, the poor long term stability of the liquid electrolyte obstructs their practical applications. An efficient way to prevent the volatility is to use the quasi solid state polymer gel electrolyte. However, PCE for the DSSCs assembled with polymer gel electrolytes is lower than that with liquid electrolyte [54]. Therefore, there has been a great deal of studies on the relationships between the performance of DSSCs and the properties of polymer get electrolyte to improve the PCE of the DSSCs based on polymer gel electrolyte. We have studied the DSSCs with polymers gel electrolyte and copolymer **P** as sensitizer to improve the stability of the device.

It has been reported that the minimum energy difference between the LUMO level of the organic sensitizer used in DSSCs and the conduction band of the TiO_2 must be greater than 0.2 eV for efficient electron injection into the conduction band from the excited state of the sensitizer [55]. The LUMO level or excited level (−3.45 eV) of copolymer **P** is well above the conduction band of TiO_2 (−4.2 eV), therefore the electron injection from the excited state of **P** is energetically feasible. In addition, the oxidation potential of **P** is sufficiently more positive that the standard redox potential of iodine/iodide couple (0.34 V vs Ag/Ag^+). Therefore the photo-oxidized copolymer **P** could be efficiently reduced by the iodide ions. On the basis of electrochemical properties of **P** (having cyano-acrylic acid as anchoring group), we have used copolymer **P** as organic sensitizer for the quasi solid state DSSCs.

Fig. 7 shows the absorption spectra of **P** film and **P** adsorbed into TiO_2 film. In comparison to the absorption spectra of copolymer film, the absorption on the TiO_2 film is broadened and slightly red shifted, indicating that **P** is assembled on the TiO_2 film in a monolayer state. A requirement for the metal free organic sensitizer is that it should posses any of the OH, COOH, C=O and cyano-acrylic acid groups [56] at its backbone, which are able of anchoring the TiO_2. Copolymer **P** carries cyano-acrylic acid groups in its backbone, which are responsible for transferring the electrons from the excited state of **P** into the conduction band of TiO_2.

The *J*–*V* curves for the devices based on polymer electrolyte with TBP (device "b") and without TBP (device "a") are shown in Fig. 8. Device "a" had a J_{sc} of 8.56 mA cm^{-2}, a V_{oc} of 0.68 V, a FF of 0.48, and

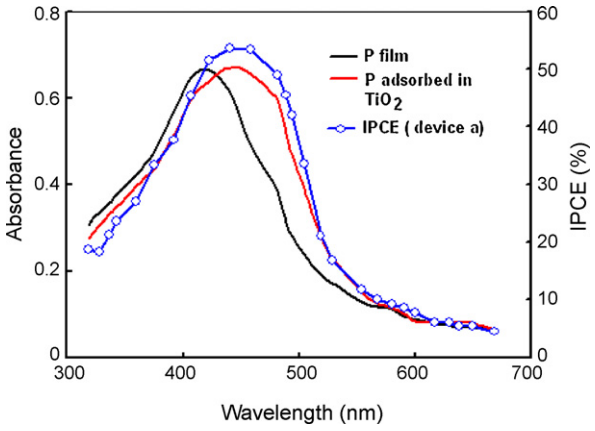

Fig. 7. UV–vis absorption spectra of **P** film, **P** adsorbed into TiO_2 film, and IPCE spectra of the device "a".

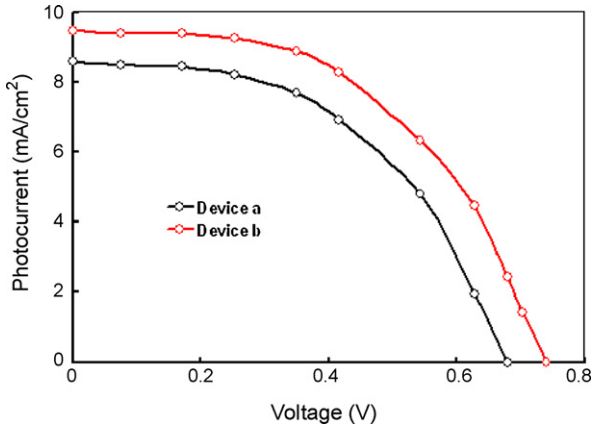

Fig. 8. Photocurrent–voltage curves of DSSCs for device "a" and "b".

overall PCE 2.8%. Improved device performance was observed for device "b", which showed a J_{sc} of 9.45 mA cm^{-2}, V_{oc} of 0.74 V, and a FF of 0.54, yielding a PCE of 3.78%. The improved PCE for the DSSCs based on electrolyte with TBP has been attributed to the negative shift in the conduction band of TiO_2 electrode and the suppression of charge recombination in the presence of TBP [57].

The incident photon to current efficiency (IPCE) spectra of the device "a" are shown in Fig. 7. The maximum IPCE is in the wavelength range of 400–500 nm, with a peak value of 54% at 458 nm, which is similar with the absorption spectrum of **P** adsorbed into TiO_2 film. This observation indicates that the photocurrent is governed by electron injection from the excited copolymer **P** through its anchoring groups, into the conduction band of TiO_2.

4. Conclusions

The Heck coupling of (*E*)-3-(4-(bis(4-bromophenyl)amino) phenyl)-2-cyanoacrylic acid with 1,4-divinyl-2,5-bis(hexyloxy)-benzene afforded copolymer **P**. The hexyloxy side chains and the non-planar structure of the TPA unit enhanced the solubility of **P**. This copolymer showed long-wavelength absorption maximum at 390–420 nm with an optical band gap of 1.94 eV. We have investigated the utility of copolymer **P** as donor for **P**:PCBM blend for the fabrication of BHJ PV device and found that the PCE is about 1.15% and 1.60% for the as cast and thermally annealed blends, respectively. The improvement in the PCE has been attributed to the increase in the crystalline nature of **P** upon thermal treatment, leading to an increase in the hole mobility. We have achieved PCE of about 2.56% and 3.48% for the devices based on the as cast and

thermally annealed **PB**:**P**:PCBM ternary blends, respectively. These values are higher than that for either **P**:PCBM or **PB**:PCBM blends which is attributed to the improvement in the light harvesting property of the blend and increased number of D/A interfaces in the BHJ active layer. Further increase in the PCE with thermally annealed ternary blend is due to the enhanced crystalline nature of both **P** and **PB**, which leads to an increase in hole mobility and better charge transport.

We have also explored the possibility of using copolymer **P** as organic sensitizer for DSSCs, and found that it is suitable as polymer sensitizer. The overall PCE for quasi solid state DSSCs based on **P** sensitizer is about 3.78%.

References

[1] B.C. Thompson, J.M.J. Frechet, Angew. Chem. Int. Ed. 47 (2008) 58.
[2] Y.J. Cheng, S.H. Yang, C.S. Hsu, Chem. Rev. 109 (2009) 5868.
[3] F.C. Krebs, M. Jørgensen, K. Norrman, O. Hagemann, J. Alstrup, T.D. Nielsen, J. Fyenbo, K. Larsen, J. Kristensen, Sol. Energy Mater. Sol. Cells 93 (2009) 422.
[4] F.C. Krebs, S. Gevorgyan, J. Alstrup, J. Mater. Chem. 19 (2009) 5442.
[5] M. Helgesen, R. Søndergaard, F.C. Krebs, J. Mater. Chem. 20 (2010) 36.
[6] F.C. Krebs, Sol. Energy Mater. Sol. Cells 93 (2009) 394.
[7] S.H. Park, A. Roy, S. Beaupre, S. Cho, N. Coates, J.S. Moon, D. Moses, M. Leclerc, K. Lee, A.J. Heeger, Nat. Photon. 3 (2009) 297.
[8] R. Qin, W. Li, C. Li, C. Du, C. Veit, H.F. Schleiermacher, M. Andersson, Z. Bo, Z. Liu, O. Ingänas, et al., J. Am. Chem. Soc. 131 (2009) 14612.
[9] Y.Y. Liang, D.Q. Feng, Y. Wu, S.T. Tsai, G. Li, C. Ray, L.P. Yu, J. Am. Chem. Soc. 131 (2009) 7792.
[10] F. Huang, K.S. Chen, H.L. Yip, S.K. Hau, O. Acton, Y. Zhang, J.D. Luo, A.K.Y. Jen, J. Am. Chem. Soc. 131 (2009) 13886.
[11] J.H. Hou, H.Y. Chen, S.Q. Zhang, R.I. Chen, Y. Yang, Y. Wu, G. Li, J. Am. Chem. Soc. 131 (2009) 15586.
[12] H.Y. Chen, J.H. Hou, S.Q. Zhang, Y.Y. Liang, G.W. Yang, Y. Yang, L.P. Yu, Y. Wu, G. Li, Nat. Photon. 3 (2009) 649.
[13] N. Blouin, A. Michaud, D. Gendron, S. Wakim, E. Blair, R. Neagu-Plesu, M. Belletete, G. Durocher, Y. Tao, M. Leclerc, J. Am. Chem. Soc. 130 (2008) 732.
[14] Y. Qin, J.Y. Kim, C.D. Frisbie, M.A. Hillmyer, Macromolecules 41 (2008) 5563.
[15] E.J. Zhou, M. Nakamura, T. Nishizawa, Y. Zhang, Q.S. Wei, K. Tajima, C.H. Yang, K. Hashimoto, Macromolecules 41 (2008) 8302.
[16] B. O' Regan, M. Grätzel, Nature 353 (1991) 737.
[17] M.K. Nazeeruddin, P. Pechy, T. Renourd, S.M. Zakeeruddin, R. Humphry-Baker, P. Comte, P. Liska, L. Cevery, E. Costa, V. Shklover, L. Spiccia, G.B. Deacon, C.A. Bignozzi, M.J. Grätzel, Am. Chem. Soc. 123 (2001) 1613.
[18] (a) K. Srinivas, K. Yesudas, K. Bhanuprakash, V.J. Rao, L.J. Giribabu, Phys. Chem. C 113 (2009) 20117;
(b) L. Giribabu, Ch.V. Kumar, P.Y. Reddy, J.-H. Yum, M. Grätzel, M.K.J. Nazeeruddin, Chem. Sci. 129 (2009) 75.
[19] J. Kwon, W. Lee, J.-Y. Kim, S. Noh, C. Lee, J.-I. Hong, New J. Chem. 34 (2010) 744.
[20] J.A. Mikroyannidis, M.M. Stylianakis, P. Suresh, P. Balraju, G.D. Sharma, Org. Electron. 10 (2009) 1320.
[21] K. Li, J. Qu, B. Xu, Y. Zhou, L. Liu, P. Peng, W. Tian, New J. Chem. 33 (2009) 2120.
[22] P. Shen, B. Zhao, X. Huang, H. Huang, S. Tan, Eur. Polym. J. 45 (2009) 2726.
[23] J.A. Mikroyannidis, Q. Dong, B. Xu, W. Tian, Synth. Met. 159 (2009) 15.
[24] Z.G. Zhang, K.-L. Zhang, G. Liu, C.-X. Zhu, K.-G. Neoh, E.-T. Kang, Macromolecules 42 (2009) 3104.
[25] G. Wu, G. Zhao, C. He, J. Zhang, Q. He, X. Chen, Y. Li, Sol. Energy Mater. Sol. Cells 113 (2009) 108.
[26] P. Shen, G. Sang, J. Lu, B. Zhao, M. Wan, Y. Zou, Y. Li, S. Tan, P. Bonhôte, J.-E. Moser, R. Humphry-Baker, N. Vlachopoulos, Macromolecules 41 (2008) 5716.
[27] S.M. Zakeeruddin, L. Walder, M. Grätzel, J. Am. Chem. Soc. 121 (1999) 1324.
[28] J. Shi, L. Wang, Y. Liang, S. Peng, F. Cheng, J. Chen, J. Phys. Chem. C 114 (2010) 6814.
[29] Y. Liang, B. Peng, J. Liang, Z. Tao, J. Chen, Org. Lett. 12 (2010) 1204.
[30] G.D. Sharma, P. Suresh, J.A. Mikroyannidis, Electochim. Acta 55 (2010) 2368.
[31] J.A. Mikroyannidis, P. Suresh, M.S. Roy, G.D. Sharma, J. Power Sources 195 (2010) 3002.
[32] W. Zhang, Z. Fang, M. Su, M. Saeys, B. Liu, Macromol. Rapid Commun. 30 (2009) 1533.
[33] J. Preat, C. Michaux, D. Jacquemin, E.A. Perpete, J. Phys. Chem. C 113 (2009) 16821.
[34] J.A. Mikroyannidis, G.D. Sharma, S.S. Sharma, Y.K. Vijay, J. Phys. Chem. C 114 (2010) 1520.
[35] D.R. McKean, G. Parrinello, A.F. Renaldo, J.K. Stille, J. Org. Chem. 52 (1987) 422.
[36] Q. Peng, M. Li, X. Tang, S. Lu, J. Peng, Y. Cao, J. Polym. Sci. Part A: Polym. Chem. 45 (2007) 1632.
[37] Z.-G. Zhang, K.-L. Zhang, G. Liu, C.-X. Zhu, K.-G. Neoh, E.-T. Kang, Macromolecules 42 (2009) 3104.
[38] S. Roquet, A. Cravino, P. Leriche, O. Alévêque, P. Frére, J. Roncali, J. Am. Chem. Soc. 128 (2006) 3459.
[39] W. Xu, B. Peng, J. Chen, M. Liang, F. Cai, J. Phys. Chem. C 112 (2008) 874.
[40] (a) V.D. Mihailetchi, P.W.M. Blom, J.C. Hummelen, M.T. Rispend, J. Appl. Phys. 94 (2003) 6849;
(b) M.C. Scharber, D. Muhlbacher, M. Koppe, P. Denk, C. Waldauf, A.J. Heeger, C.J. Brabec, Adv. Mater. 18 (2006) 789.
[41] (a) J. Peet, J.Y. Kim, N.E. Coastes, W.L. Ma, D. Moses, A.J. Heeger, G.C. Bazan, Nat. Mater. 6 (2007) 497;
(b) J. Hou, H.Y. Chen, S. Zhang, G. Li, Y. Yang, J. Am. Chem. Soc. 130 (2008) 16144;
(c) F. Zhang, J. Bijleveld, E. Perzon, K. Tvingstedt, S. Barrau, O. Ingänas, M.R. Andersson, J. Mater. Chem. 18 (2008) 5468.
[42] J.F. Chang, J. Clark, N. Zhao, H. Sirringhauss, D.W. Breiby, I. Andersen, Phys. Rev. B 74 (2006) 115318.
[43] (a) H. Hoppe, N.S. Sariciftci, J. Mater. Chem. 16 (2006) 45;
(b) J.M. Adam, M. Klaus, Adv. Funct. Mater. 16 (2009) 45.
[44] H. Sirringhaus, N. Tessler, R.H. Friend, Science 280 (1998) 1741.
[45] Y. Kim, S. Cook, S.A. Choulis, J. Nelson, J.R. Durrant, D.D.C. Bradley, Chem. Mater. 16 (2004) 4812.
[46] V.D. Mihailetchi, H. Xie, B. De Boer, L.J.A. Koster, P.W.M. Blom, Adv. Funct. Mater. 16 (2006) 699.
[47] Y. Zhao, G. Yuan, P. Roche, M. Leclerc, Polymer 36 (1995) 2211.
[48] M. Theander, O. Inaganas, W. Memmo, T. Olinga, M. Svensson, M.R. Anderson, J. Phys. Chem. B 103 (1999) 7771.
[49] W. Ma, C. Yang, X. Gong, K. Lee, A.J. Heeger, Adv. Funct. Mater. 15 (2005) 1617.
[50] J. Jo, S.S. Kim, S.I. Na, D.Y. Kim, Adv. Funct. Mater. 19 (2009) 866.
[51] V.D. Mihailetchi, L.J.A. Koster, P.W.M. Blom, Phys. Rev. Lett. 94 (2005) 126602.
[52] (a) H. Choi, C. Baik, S.O. Kang, J. Ko, M.S. Kang, M.K. Nazeeruddin, M. Grätzel, Angew. Chem. Int. Ed. 47 (2008) 327;
(b) J.A. Mikroyannidis, M.M. Stylianakis, P. Suresh, M.S. Roy, G.D. Sharma, Energy Environ. Sci. 2 (2009) 1301;
(c) W. Zhang, Z. Fang, M.J. Su, M. Saeys, B. Liu, Macromol. Rapid. Commun. 194 (2009) 1179.
[53] (a) J.K. Mwaura, X. Zhao, H. Jiang, K.S. Schanze, J.R. Reynolds, Chem. Mater. 18 (2006) 6109;
(b) X. Liu, R. Zhu, Y. Zhang, B. Liu, S. Ramakrishna, Chem. Commun. 32 (2008) 3789;
(c) C. Kanimozhi, P. Balraju, G.D. Sharma, S. Patil, J. Phys. Chem. C 114 (2010) 3095;
(d) G.D. Sharma, P. Suresh, J.A. Mikroyannidis, Synth. Met. (2010) 023, doi:10.1016/j.synthmet.2010.04.;
(e) W Zhang, Z. Fang, M. Su, M. Saeys, B. Liu, Macromol. Rapid Commun. 30 (2009) 1533.
[54] X. Zhang, H. Yang, H.M. Xiong, J. Power Sources 160 (2006) 1451.
[55] S. Ito, S.M. Zakeeruddin, R. Humphry-Baker, P. Liska, R. Charvet, P. Comte, M.K. Nazeeruddin, P. Pechy, M. Tanka, H. Mura, S. Uchida, M. Grätzel, Adv. Mater. 18 (2006) 1202.
[56] A. Mishra, M.R.K. Fishcer, P. Bauerle, Angew. Chem. Int. Ed. 48 (2009) 2474.
[57] (a) K. Hara, T. Horiguchi, T. Kinoshita, K. Sayama, H. Arakawa, Sol. Energy Mater. Sol. Cells 70 (2001) 151;
(b) S.Y. Huang, G. Schlichthori, A.J. Nozik, M. Grätzel, A.J. Frank, J. Phys. Chem. B 101 (1997) 2576.